High Frame Rate Imaging with a Small Number of Array Elements

Jian-yu Lu, *Senior Member, IEEE*, and Shiping He, *Member, IEEE*

***Abstract*—Recently, a high frame rate imaging method has been developed to construct either 2-D or 3-D images (about 3750 frames or volumes/s at a depth of about 200 mm in biological soft tissues because only one transmission is needed). The signal-to-noise ratio (SNR) is high using this method because all array elements are used in transmission and the transmit beams do not diverge. In addition, imaging hardware with the new method can be greatly simplified.**

Theoretically, the element spacing (distance between the centers of two neighboring elements) of an array should be $\lambda/2$, where λ is the wavelength, to avoid grating lobes in imaging. This requires an array of a large number of elements, especially, for 3-D imaging in which a 2-D array is needed. In this paper, we study quantitatively the relationship between the quality of images constructed with the new method and the element spacing of array transducers. In the study, two linear arrays were used. One has an aperture of 18.288 mm, elevation dimension of 12.192 mm, a center frequency of 2.25 MHz, and 48 elements (element spacing is 0.381 mm or 0.591λ). The other has a dimension of 38.4 mm $\times$ 10 mm, a center frequency of 2.5 MHz, and 64 elements (0.6 mm or 1.034λ element spacing). Effective larger element spacings were obtained by combining signals from adjacent elements. Experiments were performed with both the new and the conventional delay-and-sum methods. Results show that resolution of constructed images is not affected by the reduction of a number of elements, but the contrast of images is decreased dramatically when the element spacing is larger than about 2.365λ for objects that are not too close to the transducers. This suggests that an array of about 2.365λ spacing can be used with the new method. This may reduce the total number of elements of a fully sampled 128×128 array (0.5λ spacing) from 16384 to about 732 considering that the two perpendicular directions of a 2-D array are independent (ignoring the larger element spacing in diagonal directions of 2-D arrays).

I. Introduction

Limited diffraction beams are new types of beams that, in theory, can propagate to an infinite distance without spreading [1]–[7]. In practice, these beams have a large depth of field when they are produced with a finite aperture and energy [3]–[7]. Because of this property, they have applications in medical imaging [7]–[9], tissue property identification [10], blood flow velocity measurement [11], [12], nondestructive evaluation (NDE) of materials [13], communications [14], [15], and other areas such as electromagnetics [16] and optics [2], [3]. With limited diffraction beams [5], [6], [17]–[22], a high frame rate imaging method has been developed recently [23]–[25]. In this method, a plane wave pulse (broadband) is used in transmission. Echoes received with an array transducer are weighted to form limited diffraction beam responses of different parameters. The weighted signals are Fourier-transformed, interpolated, and then inversely Fourier-transformed to obtain an image. The new method has a number of advantages. First, it can achieve an ultra-high frame rate (about 3750 frames or volumes/s for biological soft tissues at a depth of 200 mm) because only one transmission is required to obtain a 2-D or 3-D image. Second, the imaging hardware can be greatly simplified (unlike the conventional delay-and-sum method [26] in which digital delays of signals and subsequent high-speed multiple-input digital summations are used, fast Fourier transform (FFT) and inverse fast Fourier transform (IFFT) [27] can be used for the new method). Third, because the entire array aperture is used in transmission and the transmitted beams do not spread over the entire region of interest in medical imaging, the signal-to-noise ratio (SNR) is relatively high [28]. In addition, because of the high frame rate, blood flow images can be constructed, and speckle noise can be reduced with nonlinear smoothing (averaging) techniques [29]–[31]. A discussion of the advantages of the high frame rate imaging method over other 3-D imaging methods such as explososcan [32] developed by the Duke University can be found in [23].

To implement the high frame rate imaging method, theoretically, an array transducer with an element spacing (distance between the centers of two adjacent elements) of about $\lambda/2$, where λ is the wavelength, is required [23], [24]. However, such an array has a large number of elements, especially, for a 2-D array in 3-D imaging (e.g., an 128×128 array has 16 384 elements) and is difficult to make because of the problems of interconnection of the array elements, cross-talk, and thick and stiff connection cable between the transducer and the imaging system. Moreover, such an array has a small clamping capacitance and high electrical impedance that reduce the SNR [33], [34].

In this paper, an experiment was performed to study the relationship between the quality of images constructed with the high frame rate imaging method and the element spacing of array transducers [35]. Results were compared with those obtained with a conventional delay-and-sum method [26]. In the study, two broadband linear array transducers were used. The first is a 48-element array with

Manuscript received July 24, 1998; accepted July 16, 1999. This work was supported in part by the grant HL 60301 from the National Institutes of Health.

The authors are with Ultrasound Laboratory, Department of Bioengineering, The University of Toledo, Toledo, Ohio 43606 (e-mail: jilu@eng.utoledo.edu).

a center frequency of 2.25 MHz, an aperture of 18.288 mm, an elevation length of 12.192 mm, and an element spacing of 0.381 mm (0.591λ). The second has 64 elements, a dimension of 38.4 mm $\times$ 10 mm, a 2.5-MHz center frequency, and an element spacing of 0.6 mm (1.034λ). The effective element spacings of these arrays were obtained by combining the received signals of an appropriate number of neighboring elements. Results show that resolution of images constructed with the high frame rate method is not affected by the element spacing. However, grating lobes of the line spread function of the imaging system increase with the element spacing, and the contrast of the images of the objects of an ATS tissue-equivalent phantom decreases dramatically when the element spacing is greater than about 2.365λ (here $z_{\min}/D > 1.58$, where $z_{\min}$ is the closest distance of the constructed images to the transducer surface and D is the aperture size of transducer). Because the two perpendicular directions along a 2-D array transducer are orthogonal and independent [12], [18] (see also the simulation study of 3-D objects with a 2-D array [23]), this suggests that a 2-D array of 2.365λ element spacing can be used with the high frame rate imaging method to construct a reasonably high quality image. This reduces the number of elements from 16 384 for a fully sampled ($\lambda/2$ spacing) 128 $\times$ 128 2-D array to about 732 that can be manufactured with the current advanced array transducer and interconnection technologies. Here, we ignore the larger element spacing in diagonal directions of both fully sampled and element-reduced 2-D arrays.)

The paper is organized as follows. In Section II, the theory of the high frame rate imaging method is briefly reviewed. The experiment results are given in Sections III. In Sections IV and V, we have a brief discussion and conclusion, respectively.

II. Theoretical Preliminary

Assuming that an object is illuminated with a broadband plane wave (pulse) and that a flat 1-D or 2-D array transducer is used to receive echo signals, from limited diffraction beams such as X waves, one obtains a relationship between the Fourier transform of the backscattering coefficient of biological soft tissues and the received echo signals [23], [24]:

$$R_{k_x,k_y,k_z'}(t) = \frac{1}{2\pi}\int_{-\infty}^{\infty} \frac{A(k)T(k)H(k)}{c} F(k_x,k_y,k_z')e^{-i\omega t}dk, \quad (1)$$

where $F(k_x,k_y,k_z')$ is a spatial Fourier transform of $f(x,y,z)$ that is an object function representing the distribution of backscattering coefficients of scatterers; $A(k)$ and $T(k)$ are transfer functions of the transmit and receive beams, respectively; $k = \frac{\omega}{c}$ is a wavenumber; ω is the angular frequency; c is the speed of sound; t is time; $k_z' = k + k_z = k + \sqrt{k^2 - k_x^2 - k_y^2}$; k_x, k_y, and k_z are wavenumbers along the x, y, and z axes, respectively; and $H(k)$ is the Heaviside step function [27]

$$H\left(\frac{\omega}{c}\right) = \begin{cases} 1, & \text{if } \omega \le 0 \\ 0, & \text{if } \omega > 0. \end{cases} \quad (2)$$

If the object is 2-D, i.e., the object function $f(x,y,z)$ is not a function of y, (1) can be simplified [23], [24]:

$$R^{(2D)}_{k_x,k_z'}(t) = \frac{1}{2\pi}\int_{-\infty}^{\infty} \frac{A(k)T(k)H(k)}{c} F^{(2D)}(k_x,k_z')e^{-i\omega t}dk, \quad (3)$$

where the superscript (2D) means 2-D.

From (1) or (3), the spatial Fourier transform of the object functions can be obtained from the Fourier transform of the receive signals in terms of time. Because only one transmission is required to construct either a 2-D or 3-D image, the image construction method has a potential to achieve a very high frame rate. In addition, because the FFT or IFFT can be used, the imaging system can be greatly simplified. (No digital delays and multiple-input digital summations are needed as in a conventional digital beamformer.)

Ideally, to construct images with (1) or (3), array transducers used should have an element spacing of less or equal to one-half of the wavelength concerned [23], [24]. This requires a large number of elements for a given size of an array, especially, for 2-D arrays. An array transducer of a large number of elements may have problems as discussed in the Introduction section. However, if the number of elements is reduced, quality of constructed images may be lowered. Therefore, it is important to study the trade-off between the quality of constructed images and the number of elements (or the element spacing) of an array. The following experiments will help obtain the best compromise.

III. Experiment

In the experiment, an ATS 539 tissue-equivalent phantom[1] (Fig. 1) was used. The phantom consists of cylindrical objects of different scattering coefficients relative to the background. The contrasts of these objects are -15, -10, -5, 5, 10, and 15 dB, respectively. In addition to the cylindrical objects, there are line objects in the phantom for testing the resolution of imaging systems. The boxes around the cylindrical objects and some of the line objects are shown in Fig. 1. The phantom has a frequency-dependent attenuation of about 0.5 dB/MHz per cm and the attenuation was compensated with a time-gain control (TGC) in image constructions (see the block diagram of the data acquisition of the high frame rate method in Fig. 3 of [24]).

Two transducers were used in the experiment. One has an aperture of 18.288 mm, 2.25-MHz center frequency,

[1]ATS Laboratories, Inc., Bridgeport, CT.

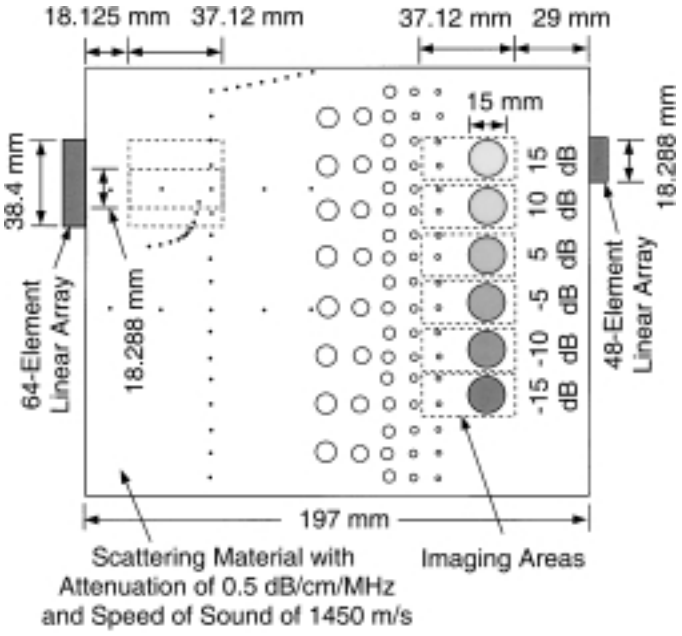

Fig. 1. A cross-section of standard ATS 539 tissue-equivalent phantom (reproduced with permission from Fig. 2 of [24]).

12.192-mm elevation dimension, an element spacing of 0.381 mm (0.591λ), and 48 total elements. The other has a dimension of 38.4 mm × 10 mm, 2.5-MHz center frequency, 0.6-mm element spacing (1.034λ), and 64 total elements. Both arrays have no focusing in the elevation direction, and the gap between elements is about 10% of the element spacing. For simplicity, no matching circuits were used, and, thus, the bandwidth (−6 dB) of the transducers is about 40% of their center frequency [24]. The speed of sound of the ATS rubber-based phantom is about 1.45 mm/μs at 23°C.

To obtain different element spacings or different numbers of elements for the arrays described previously, received signals from adjacent elements were summed. For example, to increase the element spacing from 0.591 to 1.182λ, signals from every two adjacent elements were combined.

Images constructed with the high frame rate imaging method at different element spacings are shown on the left-hand side of Fig. 2 for cross-sectional views of both cylindrical objects (see the first six columns with contrasts from 15 to −15 dB) and a line object (see the 7th and 8th columns). Images in the first seven columns were constructed with the array of 18.288 mm (aperture) and images in the 8th column were obtained with the array of 38.4 mm (aperture). The element spacings for the images in the first seven columns are 0.591, 1.182, 1.774, 2.365, 3.547, and 4.730λ, respectively, from the top to the bottom rows. Notice that the two grey-scale bars (upper and lower) on the far right of Fig. 2 have different scales, and they are used for the cylindrical and line objects, respectively. In addition, in column 8, there are only three, instead of six, images. This is because from a 64-element array, summation of signals of adjacent elements produces only arrays of an effective number of elements of 32, 16, or smaller, corresponding to an element spacing of 1.034, 2.069, and 4.138λ, respectively.

For quantitative study of the contrast of images of the cylindrical objects in Fig. 2, the following formulas were used:

$$\text{Contr} = 20 \log_{10} \left| \frac{m_i}{m_o} \right| \tag{4}$$

and

$$\text{Dev} = \left| \frac{m_i - m_o}{m_i + m_o} \right| \tag{5}$$

where m_i is the mean of the constructed image of a cylindrical object (see the circles in Fig. 2), m_o is the mean of the background of the phantom, Contr is image contrast that represents the ratio of the means inside and outside of the cylindrical objects in decibel scale, and Dev represents a mean deviation of the backscattering coefficient of a cylindrical object from that of the background. (If there is no difference between the means of the objects and the background, Dev = 0; and, if one of the means is 0 or infinity, Dev = 1; there is always $0 \leq \text{Dev} \leq 1$).

The image contrast (normalized to ±1) versus element spacing is shown in Fig. 3(1), and the deviation is shown in Fig. 4(1). It is observed that the image contrast and deviation decrease as element spacing increases.

For comparison, the same experimental data were used to construct images with the conventional delay-and-sum method [26]. The constructed images are shown on the right-hand side (from columns 9 to 16) of Fig. 2 corresponding to those on the left-hand side. The contrast and deviation of the constructed images of cylindrical objects are shown in Fig. 3(2) and 4(2), respectively.

The results in Fig. 2 to 4 show that the high frame rate imaging method produces good images as compared with the conventional delay-and-sum method. However, the high frame rate method requires many fewer computations because the FFT and IFFT can be used, which simplifies imaging systems greatly. For example, only about $N^3 \log_2 N$ computations are needed for the high frame rate method to construct a 3-D image as opposed to N^5 for the conventional method, where N is a large number. (In axial or depth dimension, N could be as large as a few thousands.) In addition, no delays of receive signals are required for the high frame rate method.

IV. Discussion

In previous sections, we have constructed images with both the high frame rate and the conventional delay-and-sum method using 1-D ultrasonic linear array transducers. Grating lobe artifacts appear in the images of wire targets for element spacings of two or more wavelengths in Fig. 2. In addition, Fig. 2 shows that grating lobes of the line spread function of the high frame rate method do

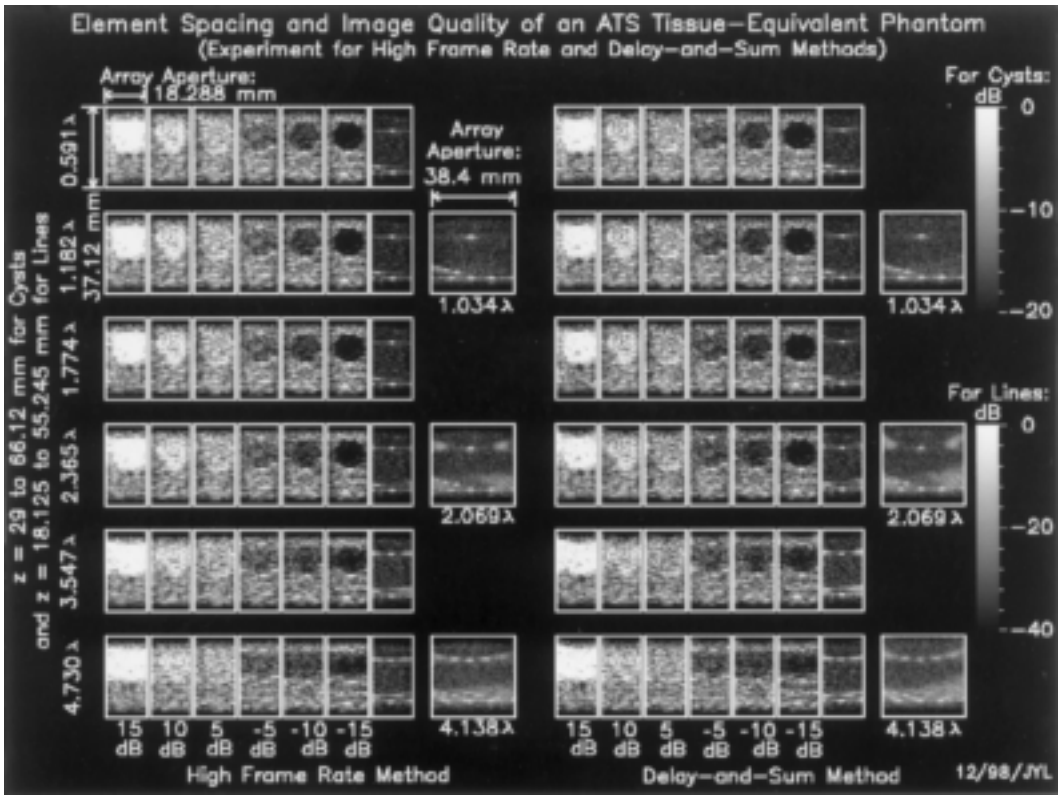

Fig. 2. Images of objects of an ATS phantom constructed experimentally with both the high frame rate and the conventional delay-and-sum [26] methods and with different element spacings. Results of the high frame rate and the conventional methods are shown in the first eight columns and the last eight columns, respectively. Images of various contrasts (15 to −15 dB) relative to the background of the phantom are shown. Images of line objects are also constructed. The element spacing for images of a smaller width (constructed with an array of 18.288 mm aperture) is from 0.591 to 4.730λ, from the top to bottom rows, respectively. Images of a larger width (constructed with an array of 38.4 mm aperture) are obtained with an element spacing from 1.034 to 4.138λ, from the top to bottom rows, respectively. Notice that the gray scale bars on the far right side are for cystic and line objects, respectively. These scales are fixed for the two types of images for comparison among images.

not affect the image contrast of cylindrical objects significantly if the element spacing is smaller than about 2.365λ. Fig. 3(1) and 4(1) show the image quality of the cysts deteriorated greatly only after the element spacing is larger than about 2.365λ. The effect of grating lobes is expected to be lessened further if images are constructed at greater depths because grating lobes may be out of the illumination area of the plane wave at these depths (notice that $z_{\min}/D$ is about 0.99 and 1.58 for images of line and cystic targets, respectively, for the array transducer of 18.288 aperture size, and z_{min}/D is about 0.47 for the 38.4-mm array). These results are valid for both image construction methods.

The resolution of images constructed with the high frame rate method is almost constant over a wide range of element spacing. This means that given an array aperture, the image resolution is almost constant.

From this study, the imaging of small specular targets (simulated by wire in a phantom) are well imaged with element spacing up to 1.77λ. For the cyst-like targets that are representative of a more frequently occurring practical medical imaging situation, the high frame rate method can be used with array transducers with an element spacing of about 2.365λ without significantly degrading the quality of constructed images. This is caused by the difference in the $z_{\min}/D$ values of the two groups of images. These results indicate that the number of array elements can be reduced significantly. For example, a fully sampled (element spacing is $\lambda/2$) 128×128 2-D array has 16 384 elements. Such an array and its imaging systems are difficult to make with the current technology. With an element spacing of 2.365λ and considering that the two perpendicular directions of a 2-D array are independent, the number of elements can be reduced to about 732 and the 2-D array can be constructed with current array technology (assuming that the larger element spacing in diagonal directions of both the fully sampled and the element-reduced 2-D arrays can be ignored).

V. Conclusion

A high frame rate imaging method is recently developed that can be used to construct images at a high frame or volume rate (about 3750 frames/s at a depth of about 200 mm in biological soft tissues), in addition to many other advantages of the new method [23]–[25]. In this paper, experiments were performed to study the relationship

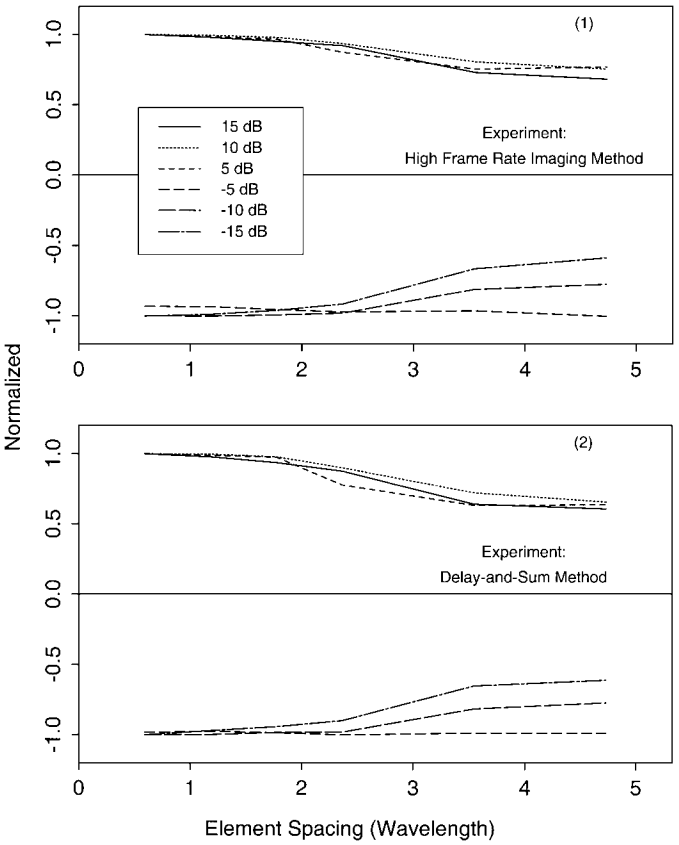

Fig. 3. Normalized contrast as a function of the element spacing of the arrays for various cylindrical objects (see Fig. 2) constructed with (1) the high frame rate and (2) delay-and-sum methods.

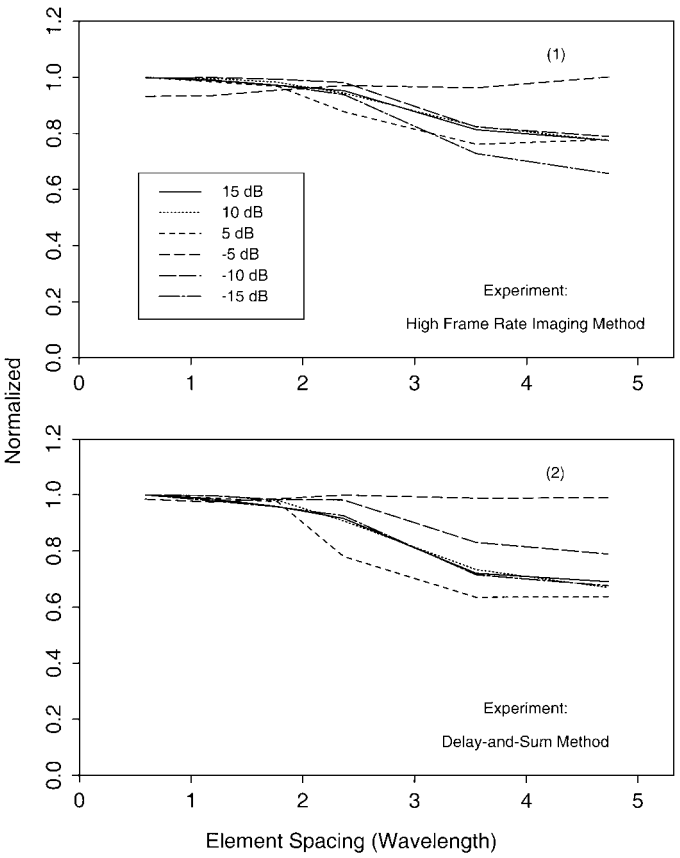

Fig. 4. Normalized deviation of images constructed with (1) high frame rate and (2) delay-and-sum methods.

between the quality of images constructed with the high frame rate method and the element spacing of array transducers. Results show that array transducers of element spacing as large as 2.365λ can be used to construct images of good quality if the object is not too close to the transducer surface (see Fig. 1 and 2). This could reduce the number of elements of a fully sampled 128×128 2-D array from 16 384 to about 732, and, thus, imaging systems with the high frame rate method can be greatly simplified.

References

[1] J. A. Stratton, *Electromagnetic Theory*. New York: McGraw-Hill Book Company, 1941, p. 356.

[2] J. Durnin, "Exact solutions for nondiffracting beams. I. The scalar theory," *J. Opt. Soc. Amer. A*, vol. 4, no. 4, pp. 651–654, 1987.

[3] J. Durnin, J. J. Miceli, Jr., and J. H. Eberly, "Diffraction-free beams," *Phys. Rev. Lett.*, vol. 58, no. 15, pp. 1499–1501, Apr. 1987.

[4] Jian-yu Lu and J. F. Greenleaf, "Ultrasonic nondiffracting transducer for medical imaging," *IEEE Trans. Ultrason., Ferroelect., Freq. Contr.*, vol. 37, no. 5, pp. 438–447, Sep. 1990.

[5] ——, "Nondiffracting X waves — exact solutions to free-space scalar wave equation and their finite aperture realizations," *IEEE Trans. Ultrason., Ferroelect., Freq. Contr.*, vol. 39, no. 1, pp. 19–31, Jan. 1992.

[6] ——, "Experimental verification of nondiffracting X waves," *IEEE Trans. Ultrason., Ferroelect., Freq. Contr.*, vol. 39, no. 3, pp. 441–446, May 1992.

[7] Jian-yu Lu, Hehong Zou, and J. F. Greenleaf, "Biomedical ultrasound beam forming," *Ultrasound Med. Biol.*, vol. 20, no. 5, pp. 403–428, Jul. 1994.

[8] Jian-yu Lu and J. F. Greenleaf, "Pulse-echo imaging using a nondiffracting beam transducer," *Ultrasound Med. Biol.*, vol. 17, no. 3, pp. 265–281, May 1991.

[9] ——, "Diffraction-limited beams and their applications for ultrasonic imaging and tissue characterization," in *New Developments in Ultrasonic Transducers and Transducer Systems*, F. L. Lizzi, Ed., pp. 92–119.

[10] ——, "Evaluation of a nondiffracting transducer for tissue characterization," *IEEE 1990 Ultrason. Symp. Proc.*, vol. 2, pp. 795–798.

[11] Jian-yu Lu, Xiao-Liang Xu, Hehong Zou, and J. F. Greenleaf, "Application of Bessel beam for Doppler velocity estimation," *IEEE Trans. Ultrason., Ferroelect., Freq. Contr.*, vol. 42, no. 4, pp. 649–662, Jul. 1995.

[12] Jian-yu Lu, "Improving accuracy of transverse velocity measurement with a new limited diffraction beam," in *IEEE 1996 Ultrason. Symp. Proc.*, vol. 2, pp. 1255–1260.

[13] Jian-yu Lu and J. F. Greenleaf, "Producing deep depth of field and depth-independent resolution in NDE with limited diffraction beams," *Ultrason. Imag.*, vol. 15, no. 2, pp. 134–149, Apr. 1993.

[14] Jian-yu Lu and Shiping He, "Optical X waves communications," *Optics Communications*, vol. 161, pp. 187–192, Mar. 1999.

[15] Jian-yu Lu, "High-speed transmissions of images with limited diffraction beams," in *Acoustical Imaging*, vol. 23, S. Lees and L. A. Ferrari, Ed., New York: Prenum Press, 1997, pp. 249-254.

[16] J. Ojeda-Castaneda and A. Noyola-lglesias, "Nondiffracting wavefields in grin and free-space," *Microwave Opt. Technol. Lett.*, vol. 3, no. 12, pp. 430–433, Dec. 1990.

[17] Jian-yu Lu and J. F. Greenleaf, "Theory and acoustic experiments of nondiffracting X waves," in *IEEE 1991 Ultrason. Symp. Proc.*, vol. 2, pp. 1155–1159.

[18] Jian-yu Lu, "Limited diffraction array beams," *Int. J. Imaging System Technol.*, vol. 8, no. 1, pp. 126–136, Jan. 1997.
[19] ——, "Designing limited diffraction beams," *IEEE Trans. Ultrason., Ferroelect., Freq. Contr.*, vol. 44, no. 1, pp. 181–193, Jan. 1997.
[20] Jian-yu Lu and J. F. Greenleaf, "Sidelobe reduction for limited diffraction pulse-echo systems," *IEEE Trans. Ultrason., Ferroelect., Freq. Contr.*, vol. 40, no. 6, pp. 735–746, Nov. 1993.
[21] Jian-yu Lu, "Bowtie limited diffraction beams for low-sidelobe and large depth of field imaging," *IEEE Trans. Ultrason., Ferroelect., Freq. Contr.*, vol. 43, no. 6, pp. 1050–1063, 1995.
[22] ——, "Producing bowtie limited diffraction beams with synthetic array experiment," *IEEE Trans. Ultrason., Ferroelect., Freq. Contr.*, vol. 42, no. 5, pp. 893–900, 1996.
[23] ——, "2D and 3D high frame rate imaging with limited diffraction beams," *IEEE Trans. Ultrason., Ferroelect., Freq. Contr.*, vol. 44, no. 4, pp. 839–856, Jul. 1997.
[24] ——, "Experimental study of high frame rate imaging with limited diffraction beams," *IEEE Trans. Ultrason., Ferroelect., Freq. Contr.*, vol. 45, no. 1, pp. 84–97, Jan. 1998.
[25] ——, "Transmit-receive dynamic focusing with limited diffraction beams," in *IEEE 1997 Ultrason. Symp. Proc.*, vol. 2, pp. 1543–1546.
[26] J. Shen, H. Wang, C. Cain, and E. S. Ebbini, "A post-beamforming processing technique for enhancing conventional pulse-echo ultrasound imaging contrast resolution," in *IEEE 1995 Ultrason. Symp. Proc.*, vol. 2, pp. 1319–1322.
[27] R. Bracewell, *The Fourier Transform and its Applications.* New York, NY: McGraw-Hill Book Company, 1965, ch. 4 and 6.
[28] Jian-yu Lu, "A study of signal-to-noise ratio of the Fourier method for construction of high frame rate images," unpublished.
[29] G. E. Trahey, S. M. Hubbard, and O. T. von Ramm, "Angle independent ultrasonic blood flow detection by frame-to-frame correlation of B-mode images," *Ultrasonics*, vol. 26, pp. 271–276, 1988.
[30] G. E. Trahey, S. W. Smith, and O. T. von Ramm, "Speckle reduction in medical ultrasound via spatial compounding," *SPIE Medicine XIV PACS,* vol. IV, pp. 626–637, 1986.
[31] S. D. Silverstein and M. O'Donnell, "Frequency and temporal compounding of partially correlated signals: Speckle suppression and image resolution," in *SPIE, Visual Communications and Image Processing II*, vol. 845, pp. 188–194, 1987.
[32] D. P. Shattuck, M. D. Weinshenker, S. W. Smith, and O. T. von Ramm, "Explososcan: A parallel processing technique for high speed ultrasound imaging with linear phased arrays," *J. Acoust. Soc. Amer.*, vol. 75, no. 4, pp. 1273–1282, 1984.
[33] L. J. Busse and D. R. Dietz, "Coherent array imaging with sparse circular array methods, performance, and application to intravascular imaging," in *IEEE 1991 Ultrason. Symp. Proc.*, vol. 1, pp. 641–644.
[34] G. R. Lockwood and F. S. Foster, "Optimizing sparse two-dimensional transducer arrays using an effective aperture approach," *IEEE 1994 Ultrason. Symp. Proc.*, vol. 2, pp. 1497–1501.
[35] Jian-yu Lu and Shiping He, "Reducing number of elements of transducer arrays in Fourier image construction method," in *IEEE 1998 Ultrason. Symp. Proc.*, vol. 2, pp. 1619–1622.

Jian-yu Lu (S'86–M'88–SM'99) was born in Fuzhou, Fujian Province, People's Republic of China. He received the B.S. degree in electrical engineering in February 1982 from Fudan University, Shanghai, China; the M.S. degree in 1985 from Tongji University, Shanghai, China; and the Ph.D. degree in 1988 from Southeast University, Nanjing, China.

He is currently a professor in the Department of Bioengineering at the University of Toledo, Toledo, Ohio, and an adjunct Professor of Medicine at the Medical College of Ohio, Toledo. Before joining the University of Toledo as a professor in September 1997, he was an associate professor of biophysics at the Mayo Medical School and an associate consultant at the Department of Physiology and Biophysics, Mayo Clinic/Foundation, Rochester, Minnesota. From March 1990 to December 1991, he was a research associate at the Department of Physiology and Biophysics, and, from December 1988 to February 1990, he was a postdoctoral research fellow there. Prior to that, he was a faculty member of the Department of Biomedical Engineering, Southeast University, Nanjing, China, and worked with Prof. Yu Wei. His research interests are in acoustic imaging and tissue characterization, medical ultrasonic transducers, and ultrasonic beam forming and propagation.

Dr. Lu is a recipient of the Outstanding Paper Award for two papers published in the 1992 *IEEE Transactions on the UFFC* and the recipient of the Edward C. Kendall Award from the Mayo Alumni Association, Mayo Foundation in 1992. He also received both the FIRST Award from the NIH and the Biomedical Engineering Research Grant Award from the Whitaker Foundation in 1991. He is a senior member of the IEEE UFFC Society and the American Institute of Ultrasound in Medicine and a member of Sigma Xi and other societies.

Shiping He (M'88) received the B. Eng., M. Eng. and Ph. D degrees from Southeast University, in 1982, 1984, and 1989, respectively. From 1989 to 1991, he was a post doctoral fellow at Nanjing University, PR China. From 1991 to 1994, he was an associate professor and a professor at Nanjing University, PR China. From 1994 to 1995, he was a senior engineer at China United Communications Corporation, Anhui Branch, PR China. Since 1995, he has been Professor and Dean of the College Electronic Engineering and the Assistant President of Anhui University, PR China. From 1996 to 1998, he was a visiting professor then post doctoral fellow at Communications Research Laboratory, McMaster University, Ontario, Canada.

Dr. He is currently a post doctoral Fellow in the Department of Bioengineering at the University of Toledo, Toledo, Ohio. Dr. He's research interests include acoustic imaging, medical ultrasonic transducers, beam forming, signal processing, cellular digital communication systems, and smart antennas for wireless personal communications that include spatial processing for CDMA systems.